JOURNAL OF SOLID STATE CHEMISTRY 114, 265–270 (1995)

A Study of the Nonstoichiometry and Physical Properties of the Perovskite $Nd_{1-x}Ca_xFeO_{3-y}$ System

Chul Hyun Yo, Ile Young Jung, Kwang Hyun Ryu, Kwang Sun Ryu, and Jin Ho Choy*

*Department of Chemistry, Yonsei University, Seoul 120-749, Korea; and *Department of Chemistry, Seoul National University, Seoul 151-742, Korea*

Received January 18, 1994; in revised form May 16, 1994; accepted May 18, 1994

A series of samples of the perovskite $Nd_{1-x}Ca_xFeO_{3-y}$ system with the compositions $x = 0.00$, 0.25, 0.50, 0.75, and 1.00 has been prepared at 1150°C under atmospheric air pressure. In the perovskite system, the X-ray powder diffraction patterns assign the compositions $x = 0.00$ and 0.25 to the orthoferrite-type orthorhombic system, the composition $x = 0.50$ to the cubic system, and the compositions $x = 0.75$ and 1.00 to the brownmillerite-type orthorhombic system. The mole ratio of Fe^{4+} ions to total Fe ions, or τ value, has been determined and identified by Mohr salt titration and Mössbauer spectroscopic analysis. Except for the compositions $x = 0.00$ and 1.00, the samples contained the mixed valence state between Fe^{3+} and Fe^{4+}, and the composition $x = 0.50$ had the maximum τ value. Nonstoichiometric chemical formulas of the system are formulated from the x, τ, and y values. The Mössbauer spectrum of $x = 0.50$ exhibits a sharp peak due to rapid electron transfer between the Fe^{3+} and Fe^{4+} ions. The electrical conductivity increases with the number of Fe^{4+} ions because the e_g-electron hole of the Fe^{4+} ion acts as a positive hole. Since the Fe^{4+} ions decrease the magnitude of the antiferromagnetic interaction of Fe^{3+}–O^{2-}–Fe^{3+}, the Néel temperature of the system decreases with increasing values of τ.

INTRODUCTION

Recently the perovskite compounds have been extensively studied due to their unique and interesting properties and many practical applications. Among these compounds, the orthoferrites with the formula $RFeO_3$, where R is a rare-earth element, have also been often investigated regarding their structural and magnetic properties (1–3).

The space group of $NdFeO_3$ is *Pbnm*, which is a distorted perovskite, and the crystallographic unit cell contains four equivalent iron ions (2). Their magnetic spins align in an antiparallel manner due to antiferromagnetic coupling between two neighboring Fe^{3+} ions through an oxygen ion, but they have weak ferromagnetism because of a spin canted by the zigzagging of octahedra containing the Fe ions along the c-axis (4, 5). The $Ln_{0.7}Ca_{0.3}FeO_{3-y}$ compound, which has been synthesized under high pressure, also exhibits weak ferromagnetism (6).

$Ca_2Fe_2O_5$ is an orthorhombic system and its space group is *Pcmn* (7). The unit cell consists of four unit cells of primitive perovskite cells of alternating sheets of octahedra (FeO_6) and tetrahedra (FeO_4) in the b-direction. Each iron ion is strongly antiferromagnetically coupled with its iron nearest neighbors by superexchange, resulting in a high Néel temperature, 725 K (8). From the study of the Mössbauer effects using the $^{57}Co/Rh$ source, the quadrupole splitting and isomer shift of Fe^{3+} ions in both the tetrahedra and octahedra are $\Delta E_q = 1.40$ mm s^{-1}, $\delta = 0.22$ mm s^{-1} and $\Delta E_q = 1.38$ mm s^{-1}, $\delta = 0.39$ mm s^{-1}, respectively (9). Grenier *et al.* have reported that solid solutions with $0.25 \leq y \leq 0.50$ for the $La_{1-2y}Ca_{2y}FeO_{3-y}$ system have the typical orthorhombic symmetry of an oxygen-vacancy-ordered structure (10). The $SrFeO_{3-y}$ and (La, Sr)FeO_{3-y} systems have been reported to have stable Fe^{4+} ions (11). Therefore, the electrical conductivity was increased by easy electron transfer between the Fe^{3+} and Fe^{4+} ions, and the Néel temperature was lowered by weakened antiferromagnetic coupling.

The orthoferrite, $NdFeO_3$, and the brownmillerite, $CaFeO_{2.5}$, containing only Fe^{3+} ions have been extensively studied. The $Nd_{1-x}Ca_xFeO_{3-y}$ system prepared by substituting Ca^{2+} ions in place of Nd^{3+} ions has not been studied systematically. Solid solutions of the $Nd_{1-x}Ca_xFeO_{3-y}$ ($x = 0.00$, 0.25, 0.50, 0.75, and 1.00) system were prepared and the cell parameters were determined by powder X-ray diffraction. The mixed valence state between Fe^{3+} and Fe^{4+} was analyzed and identified by Mohr salt titration and Mössbauer spectroscopy. The nonstoichiometric chemical formulas of the $Nd_{1-x}Ca_xFe^{3+}_{1-\tau}Fe^{4+}O_{3-y}$ ($y = (x - \tau)/2$) system were formulated from the x, τ, and y values. In order to investigate the change in physical properties caused by the formation of Fe^{4+} ions, the temperature dependencies of the electrical conductivity and magnetic susceptibility were measured. The conduction mechanism, the configuration of the magnetic spins, and the valence state of the Fe ions are discussed along with the measurements.

0022-4596/94 $6.00

TABLE 1
Lattice Parameters, Reduced Lattice Volume, and Crystal System of the $Nd_{1-x}Ca_xFeO_{3-y}$ Solid Solutions

	Lattice parameters (Å)				
x	a	b	c	V_{red}(Å^3)	Crystal system
0.00	5.585(3)	5.452(1)	7.748(1)	58.984	Orthorhombic
0.25	5.540(8)	5.392(7)	7.756(1)	57.937	Orthorhombic
0.50	3.836(1)	—	—	56.451	Cubic
0.75	5.432(3)	11.33(3)	5.570(4)	57.156	Orthorhombic
1.00	5.431(8)	14.76(3)	5.606(1)	56.193	Orthorhombic

EXPERIMENTAL

The starting materials for the samples, such as spectroscopically pure Nd_2O_3, $CaCO_3$, and $Fe(NO_3)_3 9H_2O$, were weighed in the desired proportions and dissolved in nitric acid. The solution was evaporated in a sand bath and then fired at 880°C for 6 hr in a platinum crucible. After being ground and then heated at 1150°C in air for 24 hr, the samples were weighed and analyzed by X-ray diffraction. In order to obtain a homogeneous solid solution this process was repeated until the weight and the X-ray diffraction patterns of each sample no longer varied. Each powder sample was pressed into a pellet under a pressure of 3 tonne/cm^2, and then the pellets were sintered under the same preparation conditions as for the experiments measuring electrical conductivity.

X-ray diffraction analysis of the samples was carried out by Ni-filtered Cu$K\alpha$ radiation in the range $15° \leq 2\theta \leq 80°$. Comparing the d_{obs} value from the X-ray analysis to the d_{cal} value, we confirmed the Miller indices of each line and then determined the lattice parameters, reduced lattice volume, and crystal system of the $Nd_{1-x}Ca_xFeO_{3-y}$ solid solutions as listed in Table 1. The Mohr salt analysis (12, 13) was applied to determine the number of Fe^{4+} ions or the τ value. The nonstoichiometric oxygen content, or the y value ($y = (x - \tau)/2$), should also be determined from the x and τ values. The Mössbauer spectroscopic analysis of the samples with ^{57}Fe was carried out at room temperature using a ^{57}Co/Rh source. The velocity was calibrated using Fe foil as the standard material. The spectra are fitted to the sum of Lorentzian curves by a least-squares refinement. Electrical conductivity of the samples was measured by the four-probe method in the temperature range −150 to 600°C under air pressure and calculated by the Laplume equation. Magnetic susceptibilities were measured by the Faraday method and SQUID (superconducting quantum interference device) in the temperature ranges 300 to 800 K and 4 to 300 K, respectively (14).

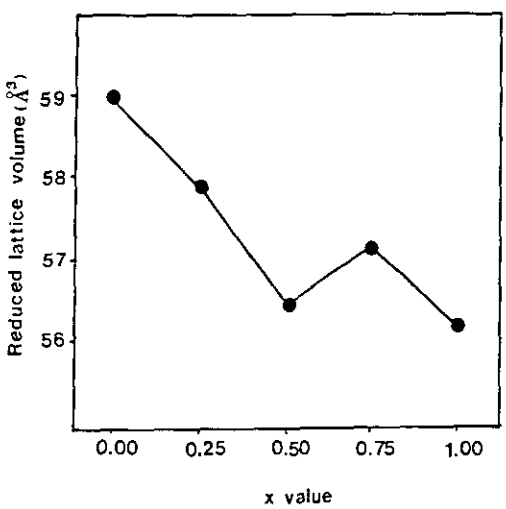

FIG. 1. Plot of the reduced lattice volume vs x value for the $Nd_{1-x}Ca_xFeO_{3-y}$ system.

RESULTS AND DISCUSSION

It is confirmed that the Nd^{3+} ions are replaced by Ca^{2+} ions in all the compositions which are homogeneous. The X-ray diffraction analysis assigns the structure of the compositions $x = 0.00$ and 0.25 to the orthorhombic system with a distorted perovskite-type structure, the composition $x = 0.50$ to the cubic system, and the compositions $x = 0.75$ and 1.00 to the brownmillerite-type orthorhombic system with ordered oxygen vacancies. The lattice parameters, reduced lattice volume, and crystal system of the compositions are listed in Table 1. The reduced lattice volume given as a function of the x value in the $Nd_{1-x}Ca_xFeO_{3-y}$ system is shown in Fig. 1. In this system, the decreasing lattice volume is mainly affected by the factor of substitution of the Ca^{2+} ions (2, 15). An abnormal decrease of the volume for $x = 0.50$ is ascribed to the 43 mole% of Fe^{4+} ion or the highest τ value. As the number of Fe^{4+} ions is increased, the bond length of Fe–O is decreased due to increased covalency between the Fe and oxygen ions.

Mohr salt analysis as listed in Table 2 shows that the compositions $x = 0.00$ and 1.00 contain only Fe^{3+} ions and the other compositions present a mixed valence state between Fe^{3+} and Fe^{4+}. The mole ratio of Fe^{4+} ions to

TABLE 2
x, τ, and y values and Nonstoichiometric Chemical Formulas of the $Nd_{1-x}Ca_xFe^{3+}_{1-\tau}Fe^{4+}_{\tau}O_{3-y}$ System

x	τ	y	Nonstoichiometric chemical formula
0.00	0.00	0.00	$NdFe^{3+}O_{3.00}$
0.25	0.09	0.08	$Nd_{0.75}Ca_{0.25}Fe^{3+}_{0.91}Fe^{4+}_{0.09}O_{2.92}$
0.50	0.43	0.03	$Nd_{0.50}Ca_{0.50}Fe^{3+}_{0.57}Fe^{4+}_{0.43}O_{2.97}$
0.75	0.08	0.33	$Nd_{0.25}Ca_{0.75}Fe^{3+}_{0.92}Fe^{4+}_{0.09}O_{2.67}$
1.00	0.00	0.50	$CaFe^{3+}O_{2.50}$

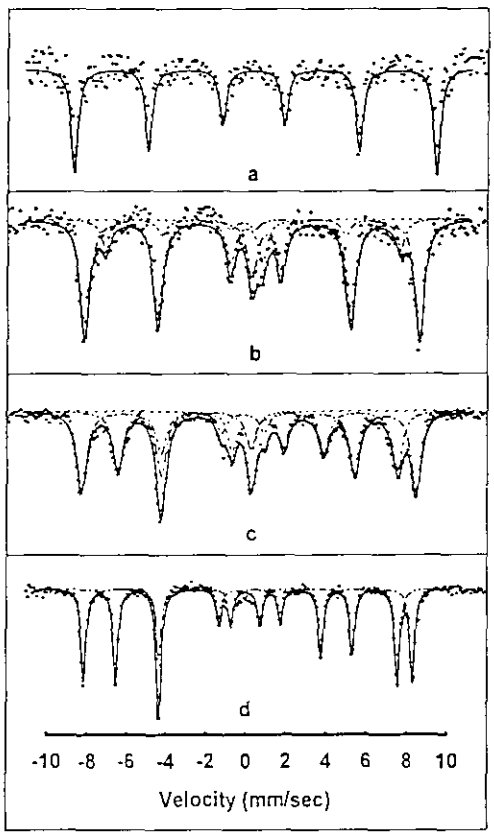

FIG. 2. Mössbauer spectra for the $Nd_{1-x}Ca_xFeO_{3-y}$ system at room temperature: (a) $NdFeO_{3.00}$, (b) $Nd_{0.75}Ca_{0.25}FeO_{2.92}$, (c) $Nd_{0.25}Ca_{0.75}FeO_{2.67}$, and (d) $CaFeO_{2.50}$.

total Fe ions, or the τ value, is maximized in the system at the composition of $x = 0.50$. It was reported that the quantity of Fe^{4+} ions increases steadily with the x value in the study of $Sr_xDy_{1-x}FeO_{3-y}$(2). However, when the Ca^{2+} ions are substituted into the A-site, the formation of oxygen vacancies is more predominant than that of Fe^{4+} ions. Therefore, the τ value increases with the x value for compositions of $0.00 \leq x \leq 0.50$ and then decreases again for compositions of $x > 0.50$. The nonstoichiometric formulas of the $Nd_{1-x}Ca_xFe^{3+}_{1-\tau}Fe^{4+}_{\tau}O_{3-y}$ system are reasonably set up from the x, τ, and y values.

The Mössbauer spectra of the $Nd_{1-x}Ca_xFeO_{3-y}$ system are shown in Figs. 2 and 3, and parameters such as isomer shift (δ), quadrupole splitting (ΔE_Q), and internal magnetic field (H_{int}) are listed in Table 3. The composition $x = 0.00$, $NdFeO_{3.00}$, exhibits a six-line peak resulting from the magnetically ordered Fe^{3+} ions located in the distorted octahedral site. The distorted octahedra induce an electric field gradient at the Fe ion and then induce quadrupole splitting in the Mössbauer spectrum.

The Fe^{3+} and Fe^{4+} ions and the oxygen vacancies are, however, all found in the compositions $x = 0.25$ and 0.75. Therefore, the compounds have complex spectra due to the mixed valence state between Fe^{3+} placed in the octahedral site and tetrahedral sites, and Fe^{4+} ions in the octahedral site. Their spectra can be fitted quite satisfactorily by using two sets of magnetic hyperfine splitting and one set of two-line splitting. The relative intensities of $Fe^{3+}(o) : Fe^{4+}(o) : Fe^{3+}(t)$ in the spectra of $x = 0.25$ and 0.75 are 79 : 11 : 10 and 54 : 10 : 36, respectively. These agree well with the result of Mohr salt analysis. As indicated by the isomer shift and hyperfine splitting, the Fe^{4+} ions are located in the octahedral site only and the Fe^{3+} ions are distributed between the octahedral and tetrahedral sites. The spectrum of the composition $x = 1.00$ shows that the sample contains only Fe^{3+} ions that are located in octahedral and tetrahedral sites in the ratio 50 : 50. This is deduced from the ordered structural model previously described (16, 17).

The compositions $x = 0.25$, 0.75, and 1.00 have much larger quadrupole splittings than $x = 0.00$. The tetrahedra of the Fe ions in this system may be distorted tetrahedra or trigonal pyramidal structures. Therefore, the Fe ions located in tetrahedral sites have a larger electric field gradient. These four-fold-coordinated Fe ions also induce the distortion of octahedra and increase the electric field gradient of the neighboring Fe ions. The quadrupole splitting of Fe ions located in the octahedral site increases with increasing numbers of tetrahedral sites.

The splitting lines of the Fe^{3+} and Fe^{4+} ions are not detected at room temperature in the composition $x = 0.50$, as shown in Fig. 3, though the composition contains a large number of Fe^{4+} ions. The Mössbauer spectroscopy may not identify the mixed valence state as a result of rapid electron transfer between the Fe^{3+} and Fe^{4+} ions. The Fe–O–Fe bond in the $x = 0.50$ composition seems to be linear, which is known from the XRD analysis. Therefore, the σ bonding character of e_g(Fe)–p(O)–e_g(Fe) is strengthened more than those of other samples involving a bent Fe–O–Fe bond. This allows

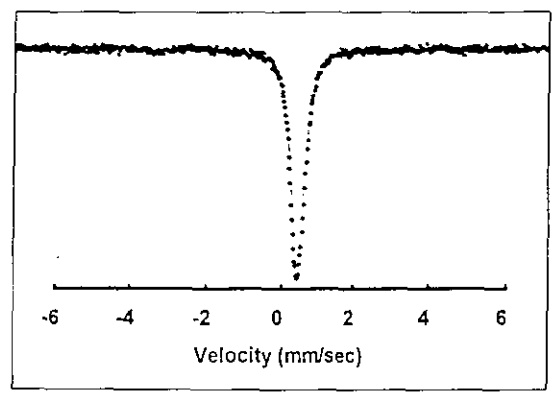

FIG. 3. Mössbauer spectra of the $Nd_{0.50}Ca_{0.50}FeO_{2.97}$ at room temperature.

TABLE 3
Valence State of the Fe Ions and Mössbauer Parameters Such as Isomer Shift, Quadrupole Splitting, and Internal Magnetic Field for the $Nd_{1-x}Ca_xFeO_{3-y}$ System

x	Fe Ion state (site)	δ(mm/sec)	ΔE_Q(mm/sec)	H_{int}(kOe)	Relative intensity (%)
0.00	Fe^{3+}(O)	0.36(2)	0.02(3)	518	100
0.25	Fe^{3+}(O)	0.38(1)	−0.16(1)	476	79
	Fe^{3+}(T)	0.21(5)	−0.10(1)	419	11
	Fe^{4+}	−0.02(2)	1.45(3)	—	10
0.50	$Fe^{3.5+}$	0.44(2)	—	—	100
0.75	Fe^{3+}(O)	0.39(3)	−0.48(3)	475	54
	Fe^{3+}(T)	0.19(3)	−0.63(3)	396	10
	Fe^{4+}	−0.15(5)	0.31(1)	—	36
1.00	Fe^{3+}(O)	0.28(5)	−0.44(3)	513	50
	Fe^{3+}(T)	0.11(3)	−0.77(3)	438	50

the rapid electron transfer between $Fe^{3+}(t_{2g}^3e_g^2)$ and $Fe^{4+}(t_{2g}^3e_g^1)$ ions. The e_g electrons of Fe^{3+} ions are transferred to the e_g orbital holes of Fe^{4+} ions. The e_g electrons of Fe ions are delocalized over the entire Fe ion, which is made possible by the indirect interaction of the Fe ions through the intervening oxygen ions. Thus the true oxidation state seems to be neither Fe^{3+} nor Fe^{4+} but an "intermediate" state.

The electrical conductivity has been shown to be a semiconducting behavior as the conductivity increases with increasing temperature, as shown in Fig. 4. At a constant temperature the electrical conductivity tends to increase with the τ value. We can find the points at which the slope of lines changes except for $x = 1.00$ in the Arrhenius plots. We could suggest that the points are associated with the magnetic transition point. The electrical activation energy varied because the spin alignment changes below the Néel temperature. The activation energy of the electrical conductivity is listed in Table 4, and the τ value and the activation energy are plotted as a function of the x value, as shown in Fig. 5.

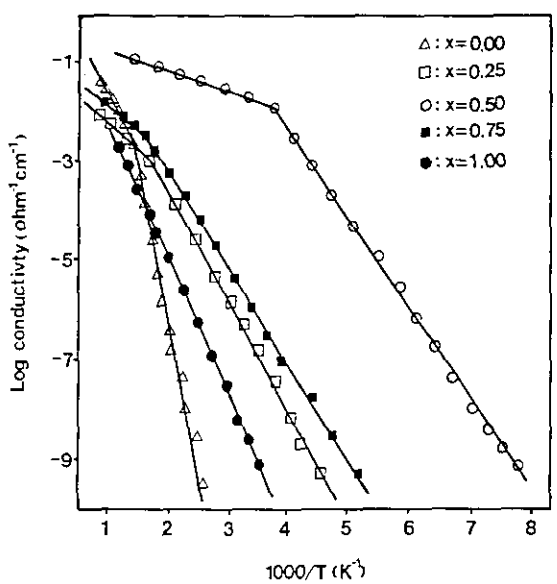

FIG. 4. Plot of log electrical conductivity vs $1000/T$ for the $Nd_{1-x}Ca_xFeO_{3-y}$ system.

The electrical conduction mechanism would be electron transfer from the Fe^{3+} ion to the e_g orbital hole of the Fe^{4+} ion through the σ bond of Fe–O–Fe. The e_g-electron hole of the Fe^{4+} ion acts as the electron acceptor. Therefore, the activation energies of the electrical conductivity for the system decrease as the τ value increases. The σ bonding character of Fe–O also affects electron transfer. In the composition $x = 0.50$ which contains a large number of Fe^{4+} ions ($\tau = 0.43$), the activation energy is very low and the electrical conductivity is higher than that of the other compositions. This is due to rapid electron transfer from the Fe^{3+} ion to the Fe^{4+} ion. It is very consistent with the results of Mössbauer spectroscopy.

The inverse of the molar magnetic susceptibilities as a function of temperature for the compositions x =

TABLE 4
Activation Energy of the Electrical Conductivity of the $Nd_{1-x}Ca_xFeO_{3-y}$ System

x	Temperature range (K)	Activation energy (eV)
0.00	$T < 700$	1.54
0.25	$T < 650$	0.46
0.50	$T < 200$	0.36
0.75	$T < 650$	0.44
1.00	$T < 700$	0.71

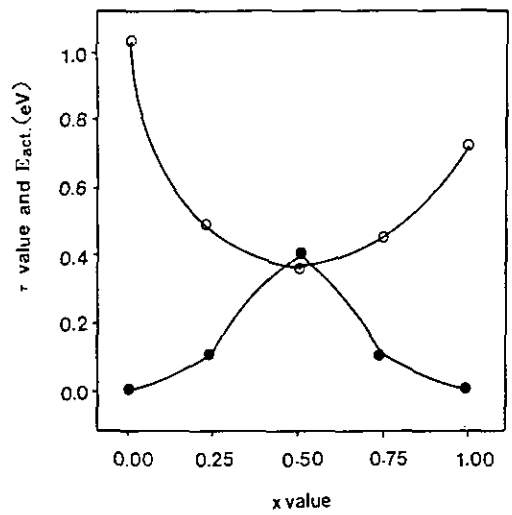

FIG. 5. Plot of τ value (closed circle) and activation energy (open circle) vs x value for the $Nd_{1-x}Ca_xFeO_{3-y}$ system.

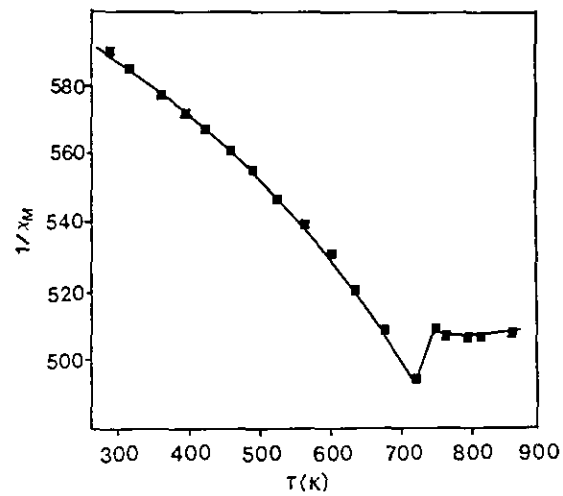

FIG. 7. Plot of $1/\chi_M$ vs absolute temperature of $CaFeO_{2.50}$.

0.00–1.00 is shown in Figs. 6 and 7. The magnetic parameters (T_N, C, and θ_p), the observed effective magnetic moment (μ_{eff}(obs)), and the calculated one (μ_{eff}(calc)) are listed in Table 5. When it is assumed that the Fe^{3+} and Fe^{4+} ions exist in the high spin state, the calculated magnetic moment is very consistent with the observed value. The electronic state of the Fe^{4+} ions is stabilized with a high spin state $t_{2g}^3e_g^1(s = 2)$ in the octahedral sites of perovskite. Therefore the electron hole of the e_g orbital affects physical properties such as the electrical and magnetic properties in nonstoichiometric perovskites.

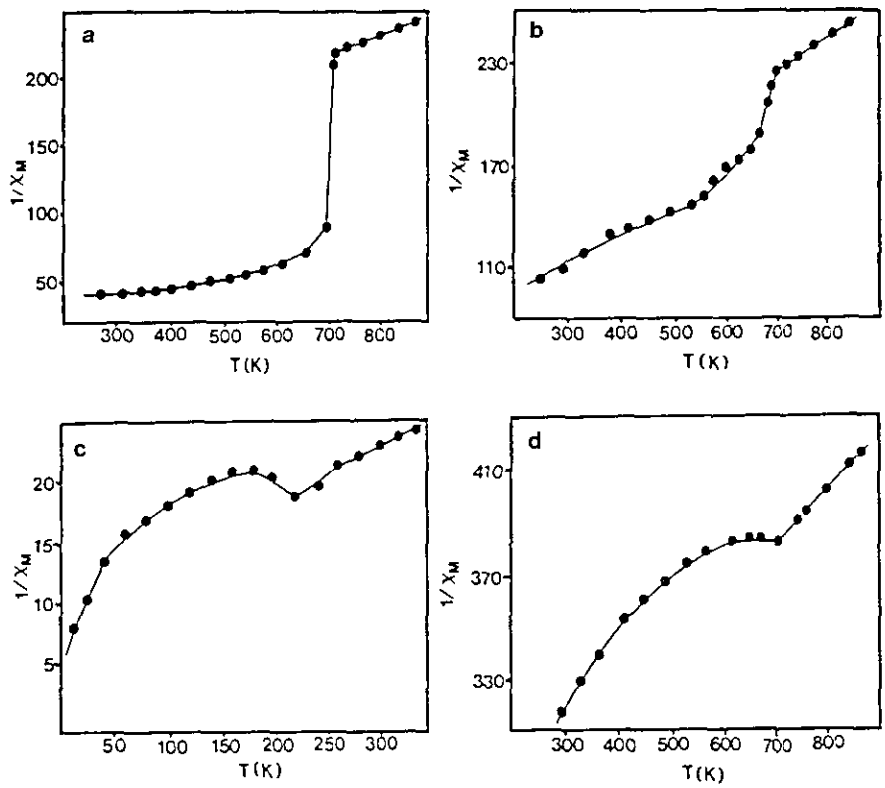

FIG. 6. Plot of $1/\chi_M$ vs absolute temperature for the $Nd_{1-x}Ca_xFeO_{3-y}$ system: (a) $NdFeO_{3.00}$, (b) $Nd_{0.75}Ca_{0.25}FeO_{2.92}$, (c) $Nd_{0.50}Ca_{0.50}FeO_{2.97}$, and (d) $Nd_{0.25}Ca_{0.75}FeO_{2.67}$.

TABLE 5
Magnetic Parameters and Observed and Calculated Effective Magnetic Moments for the $Nd_{1-x}Ca_xFeO_{3-y}$ System

x	T_N(K)	Θ_P	μ_{eff}(obs)	μ_{eff}(cal)
0.00	707	−678	5.84	5.92
0.25	680	−479	5.56	5.83
0.50	220	−394	5.43	5.50
0.75	690	−1434	5.84	5.84
1.00	720	—	—	—

The compositions $x = 0.00$ and 0.25 have a weak ferromagnetism and those where $x \geq 0.50$ have antiferromagnetism below the magnetic critical temperature. The spins of the Fe ions in the system are ordered in a direction antiparallel to each other. The weak ferromagnetism of the compositions $x = 0.00$ and 0.25 is due to spin canting by the distortion of the octahedra. It is also shown that the critical temperatures of the compositions $x = 0.25$, 0.50, and 0.75 with mixed valence states are lower than those of the stoichiometric compositions $x = 0.00$ and 1.00. This is due to the formation of the Fe^{4+} ions, which strengthens the ferromagnetic interaction between Fe^{3+} and Fe^{4+} ions and then weakens the total antiferromagnetic interaction between neighboring Fe ions.

ACKNOWLEDGMENT

This work was supported by the Korea Science and Engineering Foundation 1992 Grant 92-25-00-02 and therefore we express our appreciation to the authorities concerned.

REFERENCES

1. P. Coppens and M. Eibschutz, *Acta Crystallogr.* **19,** 524 (1965).
2. C. H. Yo, E. S. Lee, and M. S. Pyun, *J. Solid State Chem.* **73,** 411 (1988).
3. M. Takano, J. Kawachi, N. Nakanishi, and Y. Takeda, *J. Solid State Chem.* **39,** 75 (1981).
4. D. Treves, M. Eibschutz, and P. Coppens, *Phys. Lett.* **18,** 126 (1965).
5. M. Eibschutz, S. Shtrikmann, and D. Treves, *Phys. Rev.* **156,** 562 (1967).
6. I. O. Troyanchuk, A. P. Ges, S. N. Pastushonok, V. I. Pavlov, L. V. Balyco, and V. B. Shipilo, *Cryst. Res. Technol.* **24**(12), 1241 (1989).
7. J. C. Grenier, F. Menil, M. Pouchard, and P. Hagenmuller, *Mat. Res. Bull.* **13,** 329 (1978).
8. T. C. Gibb and M. Matso, *J. Solid State Chem.* **83,** 465 (1990).
9. P. R. Grenier, *Phys. Lett. A.* **35,** 413 (1971).
10. J. C. Grenier, L. Fournes, M. Pouchard, and P. Hagenmuller, *Mater. Res. Bull.* **17,** 55 (1982).
11. H. Yamamura, and R. Kuryama, *Bull. Chem. Soc. Jpn.* **45,** 2702 (1972).
12. K. S. Ryu, K. H. Ryu, K. S. Roh, and C. H. Yo, *J. Korean Chem. Soc.* **37**(11), 923 (1993).
13. C. H. Yo, K. S. Roh, S. J. Lee, K. H. Kim, and E. J. Oh, *J. Korean Chem. Soc.* **35**(3), 211 (1991).
14. R. L. Fagaly, *Sci. Prog. Oxford* **71,** 181 (1987).
15. K. H. Ryu, K. S. Roh, S. J. Lee, and C. H. Yo, *J. Solid State Chem.* **105,** 550 (1993).
16. J. C. Grenier, M. Pouchard, P. Hagenmuller, G. Schiffmacher, and P. Caro, *J. Phys.* **38,** 7(12), 84 (1977).
17. J. C. Grenier, M. Pochard, and P. Hagenmuller, "Structure and Bonding," Vol. 47, p. 2. Springer–Verlag, Berlin/Heidelberg/New York, 1981.